Kinetic roughening of magnetic flux fronts in $Bi_2Sr_2CaCu_2O_{8+\delta}$ crystals with columnar defects

D. Barness,[1,*] Y. Efraim,[2] H. Taitelbaum,[2,†] M. Sinvani,[1,‡] A. Shaulov,[1] and Y. Yeshurun[1]
[1]*Department of Physics, Institute of Superconductivity and Center for Nanotechnology, Bar-Ilan University, Ramat-Gan, 52900 Israel*
[2]*Department of Physics, Bar-Ilan University, Ramat-Gan, 52900 Israel*
(Received 6 October 2011; revised manuscript received 15 December 2011; published 14 May 2012)

Kinetic roughening analysis is utilized to investigate fingerlike flux-front patterns observed in a $Bi_2Sr_2CaCu_2O_{8+\delta}$ single crystal incorporating columnar defects. At small-length scales, scaling exponents consistent with the Kardar–Parisi–Zhang (KPZ) model for a moving front in quenched noise (QKPZ) are found. A crossover to scaling exponents of a KPZ system, dominated by temporal noise, can be identified at a large-length scale, which increases with temperature. The induction-temperature range for which the QKPZ behavior is observed is linked to the accommodation line characterizing the crossover between dominating vortex-defects and vortex-vortex interaction regimes.

DOI: 10.1103/PhysRevB.85.174516 PACS number(s): 74.25.Ha, 74.72.−h, 68.35.Fx, 89.75.Da

I. INTRODUCTION

Dynamic scaling concepts have been applied in the study of the growth of rough interfaces[1,2] in a wide range of phenomena, such as fluid flow in porous media,[3,4] propagation of flame fronts,[5] bacterial growth,[1] and flux-front propagation in superconductors (SC).[6] The growth and roughening behavior of the interfaces are characterized by a set of scaling exponents unrelated to the microscopic details of the system under investigation. This has made it possible to divide growth processes into universality classes, according to the values of these characteristic exponents.

The kinetic roughening analysis[1] is performed for segments of variable length L along the interface. Defining $h(x,t)$ as the front height at time t and location x, the interface width W, characterizing its roughness, is defined by the second moment of the fluctuations in $h(x,t)$, $W(L,t) = \sqrt{\overline{[h(x,t) - \bar{h}(t)]^2}}$, where the bar denotes a spatial average over the length L. The width is expected to scale initially as t^{β}, but after a characteristic time t_x, it should reach saturation and scale as L^{α}. The growth exponent β characterizes the dynamics of the roughening process in early times, whereas the roughness exponent α characterizes the morphology of the saturated front at long times. The crossover time t_x depends on the system size L_0 as $t_x \propto L_0^z$, where z, the dynamic exponent, is defined by the ratio $z = \alpha/\beta$. On the basis of the growth and roughness exponents, one can associate the interface dynamics with a certain universality class.

Usually, some form of disorder affects the motion of the interface leading to its roughening. Two main classes of disorder have been considered. The first, called thermal, depends only on time, whereas the second, referred to as quenched, is frozen in the medium. The Kardar–Parisi–Zhang (KPZ) model[7] considers thermal disorder, introducing a noise term $\eta(x,t)$ into the nonlinear differential equation which governs the height $h(x,t)$ of the advancing interface

$$\frac{\partial h(x,t)}{\partial t} = \upsilon \nabla^2 h + \frac{\lambda}{2}(\nabla h)^2 + \eta(x,t), \qquad (1)$$

where υ and λ are constants. This model leads to the growth exponent $\beta = 1/3$ and roughness exponent $\alpha = 1/2$. In the quenched-KPZ (QKPZ) model,[8] the thermal noise term is replaced by $\eta = \eta(x,h)$, describing a quenched noise. When the interface is pushed by a force and impeded by the medium, it fluctuates between a pinned and depinned state[9] very similar to flux motion in the presence of pinning, which results in nonlinear motion, i.e. creep.[10,11] In this case, the KPZ equation is altered by adding a driving force term F. The QKPZ model leads to $\beta = (4-d)/(4+d)$ and $\alpha = (4-d)/4$, where d is the dimension of the interface.[12] In the one-dimensional case, this leads to $\beta = 3/5$ and $\alpha = 3/4$. Another model of a growing interface in quenched disorder is the directed percolation by depinning (DPD) model, in which an interface is propagating on a square lattice with a certain fraction of forbidden sites.[13] In this model, $\alpha = \beta = 2/3$. As shown by Surdeanu *et al.*,[14] there is a strong similarity between the KPZ equation and the nonlinear diffusion equation that describes the dynamics of a vortex system, where the noise term in the latter case results both from static disorder and from thermal fluctuations.

Flux penetration in bulk SC usually forms a smooth front. Superconducting thin films, however, exhibit a vast range of nonuniform front propagations, such as macro-scale flux avalanches,[15,16] kinetic roughening,[17,18] finger patterns,[6,16] and dendrites,[19] usually ascribed to thermomagnetic instabilities.[20] Despite the rich data obtained for such phenomena, kinetic roughening analysis of the flux front in SC is hardly described in the literature. A notable exception is the work of Surdeanu *et al.*,[14] who were the first to apply dynamic scaling concepts in their study of flux-front penetration into $YBa_2Cu_3O_{7-\delta}$ thin films. Their analysis has indicated that, at small-length scales or short times, where static disorder dominates, DPD exponents are found, while at large-length scales, temporal stochastic noise dominates, and KPZ exponents are found.

In this paper, we apply kinetic roughening analysis to investigate fingerlike magnetic-flux fronts recently observed in a superconducting $Bi_2Sr_2CaCu_2O_{8+\delta}$ (BSCCO) crystal partially irradiated with heavy ions to produce a dilute concentration of columnar defects.[21] In this crystal, the smooth flux front moving in the pristine part is corrugated upon crossing the border into the irradiated part, forming fingerlike flux patterns between ∼30 and 55 K. The kinetic roughening analysis in this temperature range yields QKPZ exponents at small-length scales. A crossover to scaling exponents of a KPZ system can

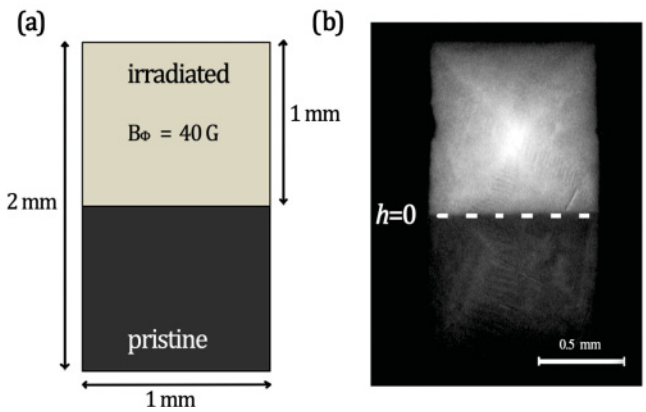

FIG. 1. (Color online) (a) Schematic diagram of the partially irradiated sample. The border across the sample center marks the location of the interface between the irradiated and pristine parts of the sample. (b) Magneto-optical image of the sample in remnant state at 24 K after a field of 1000 Oe was applied and removed. The interface between the two regions is seen to be straight and smooth. Brighter tones indicate larger B_z.

be identified at a large-length scale, indicating that while the static disorder introduced by the columnar defects dominates at small-length scales, at larger-length scales temporal stochastic noise dominates. The crossover between these two regimes occurs at a length scale which increases with temperature up to 45 K, indicating an increase in the characteristic length of regions where the quenched disorder dominates.

II. EXPERIMENTAL

A $Bi_2Sr_2CaCu_2O_{8+\delta}$ single crystal ($2 \times 1 \times 0.03$ mm^3, $T_c = 92$ K) grown by the floating zone method[22] was partially irradiated by 5 GeV Pb ions at the Grand Accelerateur National d'Ions Lourds (GANIL), Caen. The ion density during irradiation corresponded to a matching field of 40 G producing columnar defects with an average interdefect distance of $\sim$0.7 μm. The irradiated and pristine parts of this sample created two symmetrical 1×1 mm^2 regions separated by a well-defined border across the sample center, as described schematically in Fig. 1(a). Because of the fast propagation of the flux in the pristine part, the flux front reaches the border of the irradiated part when this part is essentially flux-free.

Magneto-optical (MO) images of the induction distribution normal to the sample surface $B(x,y,t)$ were taken using an iron-garnet indicator with in-plane anisotropy, and a CCD camera.[23] In a typical MO measurement, the sample was zero-field-cooled to a target temperature between 25 and 60 K and was then subjected to a field applied parallel to the crystallographic c axis of the sample and ramped up from 0 to 300 Oe at a rate $dH/dt = 0.75$ Oe/s. The pixel size defining our imaging resolution was 2×2 μm^2. We define the sharp border between the pristine and the irradiated parts as $h = 0$, and the moment at which the front reaches this border as $t = 0$. This sharp border is apparent in the magneto-optical image shown in Fig. 1(b), captured at 24 K after a 1-kOe field was applied for 10 s and then removed.

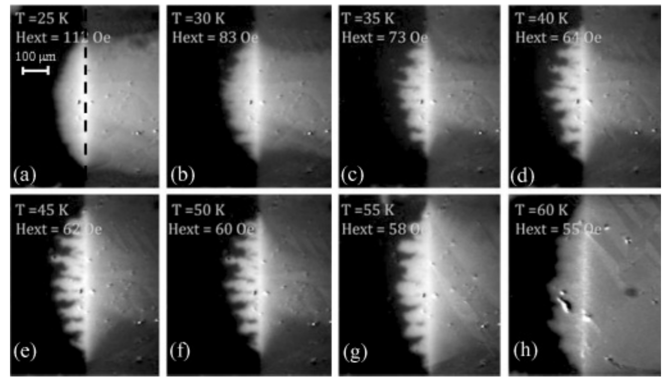

FIG. 2. Magneto-optical images of the vortex front penetrating into the irradiated region at the indicated temperatures. In all images, the right-hand side is the pristine region, and the left is the irradiated part. The dashed line in (a) marks the border between these parts. The front's structure transforms from (a) smooth to (b)–(g) fingered as temperature is increased from 25 to 55 K. (h) At higher temperatures, the fingers fade out. Images were taken at different times (different inductions) for each temperature to compare the front structures at similar distances from the irradiation border.

III. RESULTS AND DISCUSSION

Figure 2 exhibits MO images of flux penetration through the irradiation border [marked by a dashed line in Fig. 2(a)] at various temperatures, as the field is ramped up at a rate of 0.75 Oe/s. It is seen that, after crossing the border, the flux front remains uniform at 25 K (the curvature is a result of the sample geometry). However, at 30–55 K, the front exhibits a fingered pattern, and above 55 K, the fingers fade out. The time evolution of a fingered front is demonstrated by the sequence of MO images in Fig. 3. The images show the flux front as it propagates inside the irradiated region at $T = 40$ K, with a 6 s time interval between each image, starting 1 s after the initial penetration into the irradiated zone. Only the central part of the front, approximately 300 μm in length, is shown. This part, which is analyzed later, was chosen to eliminate effects of flux penetration from the sample sides in shaping the flux front. The images in Fig. 3 were cropped and rotated

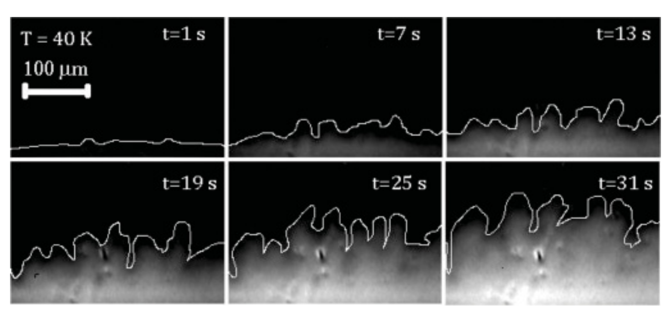

FIG. 3. Magneto-optical images of a single sequence at $T = 40$ K taken at a 6 s interval between each image. Penetration started at $t = 0$. Images were cropped to show the irradiated region only and rotated by 90° relative to the images in Fig. 2. The bottom of each image indicates the location of the irradiation border $h = 0$. White line in each image indicates shape of the digitized front $h(x)$ used for kinetic roughness analysis.

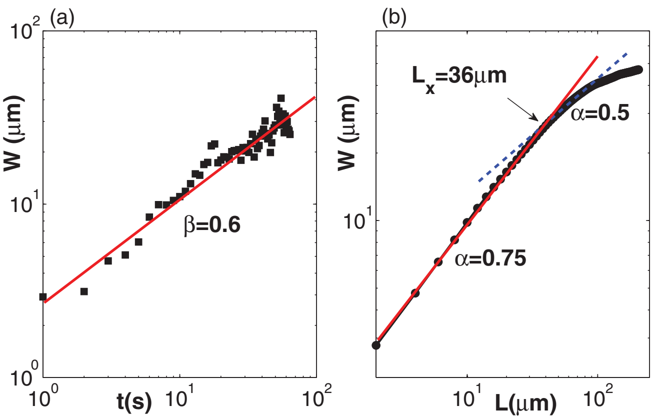

FIG. 4. (Color online) Log-log plots of the roughness W as a function of (a) time (for fixed length $L = 180\ \mu$m) and (b) scale L (at $t = 64$ s), obtained from the front roughness analysis at 40 K. The red solid lines with slopes 0.6 and 0.75 are drawn to show consistency with the scaling exponents β and α of the QKPZ model, respectively. The slope of the dashed blue line corresponds to the KPZ value $\alpha = 0.5$.

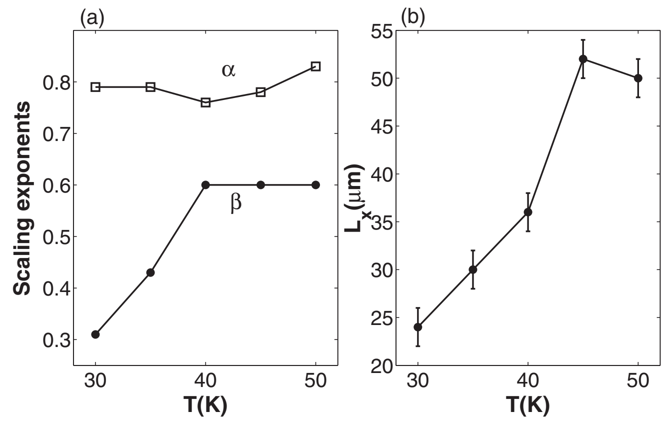

FIG. 5. (a) Temperature dependences of the scaling exponents α (open boxes) and β (full circles) and (b) of the crossover length scale L_x.

to show the relevant part of the flux front propagating upwards. The flux-front shape for each image was digitized by choosing a grey level corresponding to an induction of 5 G, close to the sensitivity limit of our detector. This line was marked for each frame of every sequence, using the image processing and analysis ImageJ program. We note that the fronts have backbends, especially at the final stages of the experiment; in the kinetic roughening analysis, we define $h(x,t)$ as the maximal value of the front at each x coordinate, as it is the real front of the process.[24,25]

Figures 4(a) and 4(b) show log-log plots of the front width W at $T = 40$ K as a function of time for $L = 180\ \mu$m and as a function of the length scale L for $t = 64$ s (above the estimated[26] $t_x \approx 60$ s), respectively. The solid red lines in Figs. 4(a) and 4(b) were drawn with slopes 0.6 and 0.75, respectively, to show consistency with the scaling exponents $\beta = 0.6$ and $\alpha = 0.75$ of the QKPZ model. These lines match fairly well with the experimental data at short times and small-length scales, indicating the dominant role of the columnar defects in shaping the flux front. The data of Fig. 4(b) deviate from the slope of 0.75 around $L_x \sim 36\ \mu$m above which one can identify a crossover to a slope of 0.5 (dashed blue line), corresponding to α in the KPZ model. Deviations from this slope above approximately $L \sim 100\ \mu$m may be ascribed to finite size effects. The length scale L_x at which the crossover between the two values of α occurs has been associated with the correlation length ξ_d of the disorder in the medium.[14,27] For length scales larger than L_x, time-dependent disorder dominates and a KPZ exponent is measured. A similar crossover was reported by Surdeanu *et al.*[14] in their kinetic roughening analysis of penetrating flux fronts in high-T_c superconducting thin films.

We further measured the temperature dependence of the scaling exponents and the crossover length of the propagating flux fronts. Figure 5(a) summarizes the temperature dependence of α and β between 30 and 50 K. While α varies only slightly (less than 10%) with temperature, the growth exponent β initially increases with temperature, up to 40 K, and then saturates. At 30 K, the exponent $\beta \sim 0.3$, indicating a rather slow progress of the front roughening. We note that the set of exponents α and β found at this temperature does not belong to any of the known universality classes. However, as the system approaches 40 K, the exponents tend to the set of exponents ($\beta = 0.6$, $\alpha = 0.75$), which, as mentioned above, associates the front dynamics with the QKPZ equation for nonlinear front evolution in quenched disorder.[12,25,28] The fact that the gross features of the front morphology are reproducible supports the argument that the front roughening is governed by the quenched noise, as expected by the QKPZ description. This description is consistent with that found in some experiments involving fronts moving in the critical state for type-II thin superconducting films.[18]

The association of the finger patterns with the quenched noise introduced by the columnar defects is further supported by the fact that, above ∼55 K, the fingered patterns disappear. This temperature is close to the depinning temperature[29–31] T_{dp}, above which the vortex-defects interaction is negligible. The depinning temperature can be estimated using the relation $T_{dp} \approx T_c\,[\kappa/(1+\kappa)]$ with $\kappa = (r_0/4\xi_{ab})(1/\sqrt{Gi})$, where $T_c = 92$ K, the columnar defect radius $r_0 = 3.5$ nm, the zero temperature coherence length in the ab plane $\xi_{ab} = 1.5$ nm, and the Ginzburg number for the 2D $Bi_2Sr_2CaCu_2O_{8+\delta}$ $Gi = 0.1$.[11,29] This yields $T_{dp} = 59$ K, setting an upper temperature limit for the QKPZ behavior.

Figure 5(b) shows that the crossover length L_x increases steadily with temperature, up to 45 K, indicating that the length scale characterizing the regions where quench disorder dominates increases with temperature. [At 50 K, there is a minor (∼2 μm = 1 pixel) decrease in L_x; however, it is not significant enough to be considered as a real change in the trend.] As indicated above, this length scale is associated with the correlation length ξ_d of the disorder in the medium. The increase of L_x with temperature reflects the increase in ξ_d as the system depinning temperature[29–31] T_{dp} is approached.

Besides the temperature upper limit, there is also an upper limit to the induction for which QKPZ behavior may be observed; at high inductions, the vortex system is dominated by the vortex-vortex interaction, and the quenched disorder

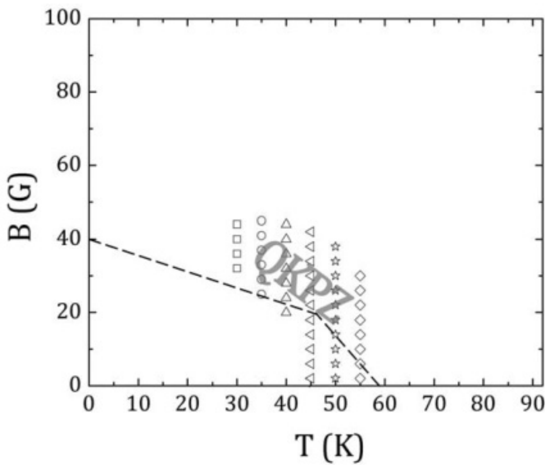

FIG. 6. Summary of the experimental results plotted in a B-T diagram. The lowest induction point for each temperature was taken on the flux front when finger patterns start to evolve. The highest induction point for each temperature was taken when no patterns could be observed. The approximated accommodation line according to the prescription of Ref. 30 is shown by the dashed lines. The points mark the inductions and temperatures for which QKPZ exponents were measured.

introduced by the columnar defects does not play a role. The limited induction-temperature (B-T) range of the QKPZ behavior is demonstrated in Fig. 6, in which the points mark the inductions and temperatures for which QKPZ exponents were measured. In these measurements, at each temperature, the sample was zero-field-cooled, and the local induction was measured on the penetrating flux front, while the external field was ramped at 0.75 Oe/s; the lowest induction point marks the first appearance of finger patterns, whereas the highest induction marks the induction beyond which the finger pattern disappears.

As proposed by Nelson and Vinokur,[32] the crossover between the regime of vortices well localized on columnar defects and the interaction dominated collective regime is described by the accommodation line, $B^*(T)$. This line may be estimated as follows:[30] B^* decreases linearly from the matching induction B_Φ (extrapolating to zero at T_c) until it reaches $\sim 0.5 B_\Phi$. From this point, it drops abruptly to zero at T_{dp}. The dashed line in Fig. 6 describes the estimated accommodation line for our sample ($T_{dp} = 59$ K, $B_\Phi = 40$ G). As apparent from the figure, all the experimental points are scattered around $B^*(T)$. In this range, on the B-T diagram, there is a fair competition between the vortex-defects and the vortex-vortex interactions, leading to the front growth according to the QKPZ model. At high temperature (or high induction), the vortex-vortex interaction is much more dominant than the vortex-defects interaction; therefore, a smooth collective propagation of the front is expected. On the other hand, at very low temperature (or low induction), the pinning effect is so pronounced that it prevents the front from developing. In the specific range of temperatures and inductions where these two interactions are comparable, the QKPZ dynamic of the front is valid, and finger pattern appears.

IV. SUMMARY

We analyzed the roughening of the magnetic flux front moving from a pristine into a heavy-ion irradiated part of a $Bi_2Sr_2CaCu_2O_{8+\delta}$ crystal. Our analysis revealed that, in a limited induction-temperature (B-T) range, the columnar defects introduced by the irradiation acted as quenched noise governing the morphology of the flux front. In this B-T range, our results are consistent with the QKPZ model. A crossover to KPZ exponents was found at a length scale L_x which increases with temperature, consistent with the expected divergence of the disorder correlation length as the depinning temperature is approached. Our findings locate the B-T regime of the QKPZ behavior near the accommodation line, characterizing the crossover between the regime of vortices well localized on columnar defects and the interaction-dominated collective regime.

ACKNOWLEDGMENTS

This research was supported by the Israel Science Foundation (ISF) Grant No. 499/07. We thank Daniel Levi for his help in various stages of this work, Yossi Bachar for extensive help in digitizing the magneto-optical front sequences, and Eli Zeldov, Baruch Rosenstein, and Rinke Wijngaarden for illuminating discussions.

[*]Present address: Elbit Systems Electro-Optics (Elop) Ltd., Rehovot, 76111 Israel.
[†]Corresponding author: haimt@mail.biu.ac.il
[‡]Present address: Faculty of Engineering, Bar-Ilan University, Ramat-Gan, 52900 Israel.

[1] A. L. Barabasi and H. E. Stanley, *Fractal Concepts in Surface Growth* (Cambridge University Press, Cambridge, 1995).
[2] P. Meakin, *Fractals, Scaling and Growth Far From Equilibrium* (Cambridge University Press, Cambridge, 1998).
[3] F. Family and T. Vicsek, eds., *Dynamics of Fractal Surfaces* (World Scientific, Singapore, 1991).
[4] M. Alava, M. Dube, and M. Rosi, Adv. Phys. **53**, 83 (2004).
[5] J. Maunuksela, M. Myllys, O. P. Kähkönen, J. Timonen, N. Provatas, M. J. Alava, and T. Ala-Nissila, Phys. Rev Lett. **79**, 1515 (1997).
[6] E. Altshuler and T. Johansen, Rev. Mod. Phys. **76**, 471 (2004).
[7] M. Kardar, G. Parisi, and Y. C. Zhang, Phys. Rev. Lett. **56**, 889 (1986).
[8] L. H. Tang, M. Kardar, and D. Dhar, Phys. Rev. Lett. **74**, 920 (1995).
[9] H. G. E. Hentschel and F. Family, Phys. Rev. Lett. **66**, 1982 (1991).
[10] P. W. Anderson, Phys. Rev. Lett. **9**, 309 (1962); M. R. Beasley, R. Labousch, and W. W. Webb, Phys. Rev. **181**, 682 (1969); Y. Yeshurun and A. P. Malozemoff, Phys. Rev. Lett. **60**, 2202 (1988).
[11] Y. Yeshurun, A. P. Malozemoff, and A. Shaulov, Rev. Mod. Phys. **68**, 911 (1996).

[12] Z. Csahók, K. Honda, E. Somfai, M. Vicsek, and T. Vicsek, Physica A **200**, 136 (1993); Z. Csahok, K. Honda, and T. Vicsek, J. Phys. A: Math. Gen. **26**, L171 (1993).

[13] S. V. Buldyrev, A. L. Barabasi, F. Caserta, S. Havlin, H. E. Stanley, and T. Vicsek, Phys. Rev. A **45**, R8313 (1992).

[14] R. Surdeanu, R. J. Wijngaarden, E. Visser, J. M. Huijbregtse, J. H. Rector, B. Dam, and R. Griessen, Phys. Rev. Lett. **83**, 2054 (1999).

[15] E. Altshuler, T. H. Johansen, Y. Paltiel, P. Jin, K. E. Bassler, O. Ramos, Q. Y. Chen, G. F. Reiter, E. Zeldov, and C. W. Chu, Phys. Rev. B **70**, 140505 (2004); P. Esquinazi, A. Setzer, D. Fuchs, Y. Kopelevich, E. Zeldov, and C. Assmann, *ibid.* **60**, 12454 (1999).

[16] E. Altshuler, T. H. Johansen, Y. Paltiel, P. Jin, K. E. Bassler, O. Ramos, G. F. Reiter, E. Zeldov, and C. W. Chu, Physica C **408**, 501 (2004).

[17] C. M. Aegerter, M. S. Welling, and R. J. Wijngaarden, Europhys. Lett. **65**, 753 (2004); Physica C **347**, 363 (2005); Europhys. Lett. **74**, 397 (2006).

[18] V. K. Vlasko-Vlasov, U. Welp, V. Metlushko, and G. W. Crabtree, Phys. Rev. B **69**, 140504 (2004).

[19] B. Biehler, B. U. Runge, P. Leiderer, and R. G. Mints, Phys. Rev. B **72**, 024532 (2005); A. V. Bobyl, D. V. Shantsev, T. H. Johansen, W. N. Kang, H. J. Kim, E. M. Choi, and S. I. Lee, Appl. Phys. Lett. **80**, 4588 (2002); C. A. Duran, P. L. Gammel, R. E. Miller, and D. J. Bishop, Phys. Rev. B **52**, 75 (1995); A. A. F. Olsen, T. H. Johansen, D. Shantsev, E. M. Choi, H. S. Lee, H. J. Kim, and S. I. Lee, *ibid.* **74**, 064506 (2006); I. A. Rudnev, S. V. Antonenko, D. V. Shantsev, T. H. Johansen, and A. E. Primenko, Cryogenics **43**, 663 (2003).

[20] M. Baziljevich, A. V. Bobyl, D. V. Shantsev, E. Altshuler, T. H. Johansen, and S. I. Lee, Physica C **369**, 93 (2002); D. V. Denisov, D. V. Shantsev, Y. M. Galperin, E. M. Choi, H. S. Lee, S. I. Lee, A. V. Bobyl, P. E. Goa, A. A. F. Olsen, and T. H. Johansen, Phys. Rev. Lett. **97**, 077002 (2006); A. L. Rakhmanov, D. V. Shantsev, Y. M. Galperin, and T. H. Johansen, Phys. Rev. B **70**, 224502 (2004).

[21] D. Barness, M. Sinvani, A. Shaulov, T. Tamegai, and Y. Yeshurun, Phys. Rev. B **77**, 094514 (2008).

[22] N. Motohira, K. Kuwahara, T. Hasegawa, K. Kishio, and K. Kitazawa, J. Ceram. Soc. Jpn. **97**, 1009 (1989).

[23] D. Giller, A. Shaulov, L. A. Dorosinskii, T. Tamegai, and Y. Yeshurun, Physica C **341**, 1089 (2000); D. Giller, A. Shaulov, T. Tamegai, and Y. Yeshurun, Phys. Rev. Lett. **84**, 3698 (2000).

[24] M. Cieplak, A. Maritan, and J. R. Banavar, J. Phys. A **27**, L765 (1994).

[25] Y. Efraim and H. Taitelbaum, Cent. Eur. J. Phys. **7**, 503 (2009)

[26] Here, t_x is estimated by plotting $W(L)$ for several times at the end of the experiment. When a stability of the morphological measure is observed, i.e. α is consistent for a certain time segment, the growth was practically ended, and saturation is achieved.

[27] L. A. N. Amaral, A. L. Barabasi, H. A. Makse, and H. E. Stanley, Phys. Rev. E **52**, 4087 (1995); L. A. N. Amaral and H. A. Makse, Phys. Rev. Lett. **80**, 5706 (1998). In these references, the correlation length diverges when the applied force F approaches its critical value F_c, above which the interface moves unaffected by pinning. In our experiment, F is approximately constant, but F_c decreases as the temperature increases toward T_{dp}.

[28] A. Be'er, I. Hecht, and H. Taitelbaum, Phys. Rev. E **72**, 031606 (2005); I. Hecht, A. Be'er, and H. Taitelbaum, Fluct. Noise Lett. **5**, 319 (2005); L. Yin, B. T. Murray, S. Su, Y. Sun, Y. Efraim, H. Taitelbaum, and T. J. Singler, J. Phys.: Condens. Matter **21** 464130 (2009).

[29] G. Blatter, M. V. Feigel'man, V. B. Geshkenbein, A. I. Larkin, and V. M. Vinokur, Rev. Mod. Phys. **66**, 1125 (1994).

[30] L. Krusin-Elbaum, L. Civale, J. R. Thompson, and C. Feild, Phys. Rev. B **53**, 11744 (1996) and references therein.

[31] L. Krusin-Elbaum, L. Civale, G. Blatter, A. D. Marwick, F. Holtzberg, and C. Feild, Phys. Rev. Lett. **72**, 1914 (1994).

[32] D. R. Nelson and V. M. Vinokur, Phys. Rev. Lett. **68**, 2398 (1992); Phys. Rev. B **48**, 13060 (1993).